processes

MDPI

Review

Research Status and Development Tendency of Salt Bath Heat Treatment of Sorbite Wire Rod

Jun Li [1,*], Chuanmin Li [1], Yafeng Liu [1], Ben Zhang [1] and Bo Wang [2]

[1] MCC Capital Engineering & Research Incorporation Limited, Beijing 100176, China
[2] School of Materials Science and Engineering, Shanghai University, Shanghai 200072, China
* Correspondence: lijun240192@ceri.com.cn

Abstract: The crucial point for obtaining high-strength wire is controlling the microstructure, and the refinement of the interlamellar spacing between 80 and 150 nm gives sorbite excellent tensile strength and plastic deformation ability. To realize sorbitization, the fastest possible cooling rate should be used to avoid austenite being transformed into coarse pearlite. In this article, the main production processes, advantages, and disadvantages of wire rods for bridges are discussed, and the relationship between microstructure and mechanical characteristics of wire rods is argued. On this basis, the research works of simulation and experiments for heat treatment of wire rods in a salt bath, together with the convection and boiling heat exchange mechanism of wire rods in a salt bath, are discussed and provided. The salt bath quenching course is capable of cooling the wire rapidly from the austenitizing temperature to the sorbite temperature region and also dissipates the latent heat, thus reducing the reheating temperature of the wires. It can realize precise control over the microstructure and characteristics of wire and has advantages in improving the wire strength, hardness, wear, and corrosion resistance. The process parameters are highly adjustable, with strong adaptability and flexibility. To obtain ultra-high-strength sorbite steel wire, the key technical problems to be solved include selecting the suitable coolant, controlling the internal microstructure, and precisely controlling the cooling effect.

Keywords: molten salt; wire rods; phase transition; heat transfer coefficient; salt bath

check for updates

Academic Editors: Qingmin Yu and Vijaya Raghavan

Received: 6 February 2025
Revised: 4 March 2025
Accepted: 8 March 2025
Published: 12 March 2025

Citation: Li, J.; Li, C.; Liu, Y.; Zhang, B.; Wang, B. Research Status and Development Tendency of Salt Bath Heat Treatment of Sorbite Wire Rod. *Processes* **2025**, *13*, 830. https://doi.org/10.3390/pr13030830

Copyright: © 2025 by the authors. Licensee MDPI, Basel, Switzerland. This article is an open access article distributed under the terms and conditions of the Creative Commons Attribution (CC BY) license (https://creativecommons.org/licenses/by/4.0/).

1. Introduction

With the development of bridge industry technology, long-span suspension bridges and cable-stayed bridges have higher requirements for the tensile strength level of their cable wires. The application of 1700 MPa grade steel wire began more than 10 years ago, such as Zhoushan Xihoumen Bridge and Ma'anshan Yangtze River Bridge [1]. Currently, the strength of 5 mm diameter hot-dip-galvanized steel wire has been developed to more than 2300 MPa. Improving the strength level of the steel wire can not only greatly improve the bearing capacity of the bridge but also reduce the weight of the bridge cable itself. Every 100 MPa increase in the tensile strength can reduce the weight of the wire by about 10% [2].

The key technology of high-strength steel wires lies in controlling the microstructure to obtain fine lamellar pearlite (sorbite) during the heat treatment process. This requires the formulation of appropriate cooling procedures and the selection of suitable cooling media. Additionally, homogenization treatment is necessary to ensure the stability and uniformity of the properties throughout the entire length of the wire.

Figure 1 shows a typical suspension bridge structure. As bridge construction develops in the direction of long-span and lightweight, ultra-high-strength, and torsional properties,

corrosion resistance and fracture resistance will become the future development direction for bridge cable steel. The crucial point for obtaining the high-strength wire is acquiring sorbite and, at the same time, homogenization treatment needs to be used to ensure the stability and uniformity of the steel wire performance.



Figure 1. Suspension bridge [2].

Based on the research status of the wire rods used in bridges and the production status of the steel industry, this article discusses the correlations between the microstructure and characteristics of high-strength wire rods and analyzes their strengthening mechanism. It is believed that salt bath heat treatment is the developing trend of high-strength wire. Its advantages, simulation and experimental research status, and future development trends are pointed out in order to provide reference for the development of ultra-high-strength wires.

2. Effects of Supercooling and Chemical Composition of Austenite on Wire Properties

2.1. Transformation Products of Supercooled Austenite and Advantages of Sorbite

As seen in Table 1, austenite can be cooled to form a variety of products. As shown in Figure 2, the sorbite has a double-layer composite microstructure with excellent tensile strength and impact toughness [3,4], the tensile strength is 700~1500 MPa, and the elongation is 10~20%, which has excellent comprehensive mechanical properties [5]. The lower the temperature of supercooled austenite transformation, the finer the interlamellar spacing (the interlamellar spacing is approximately 80 nm). The refinement of interlamellar spacing prevents the motion of the dislocations at the phase boundary. Therefore, the deformation can be spread over a large number of laminae, thus decreasing the possibility of stress concentrating and giving the wire better mechanical properties [6].

Table 1. Supercooled austenite products corresponding to different cooling ranges [7].

Transformation Type	Transformation Products	Transformation Temperature (°C)	Transformation Mechanism	Coolant	Microstructure Characteristics	Hardness (HRC)
Pearlite	Pearlite	A1~650	Diffusion type	air	Corase flakes	5~20
	Sorbite	650~600		Molten salt	Fine flakes	20~30
	Troostite	600~550		Molten salt	Extremely fine flakes	30~40
Bainite	Upper bainite	550~350	Semi diffusive type	Molten salt/oil	Feather shaped	40~50
	Lower bainite	350~230		Molten salt/oil	Bamboo leaf shaped	50~60

Table 1. *Cont.*

Transformation Type	Transformation Products	Transformation Temperature (°C)	Transformation Mechanism	Coolant	Microstructure Characteristics	Hardness (HRC)
Martensite	Acicular martensite	230~50	Non diffusive type	Water/oil	Acicular	60~65
	Lath martensite	230~50		Water/oil	Lath	50

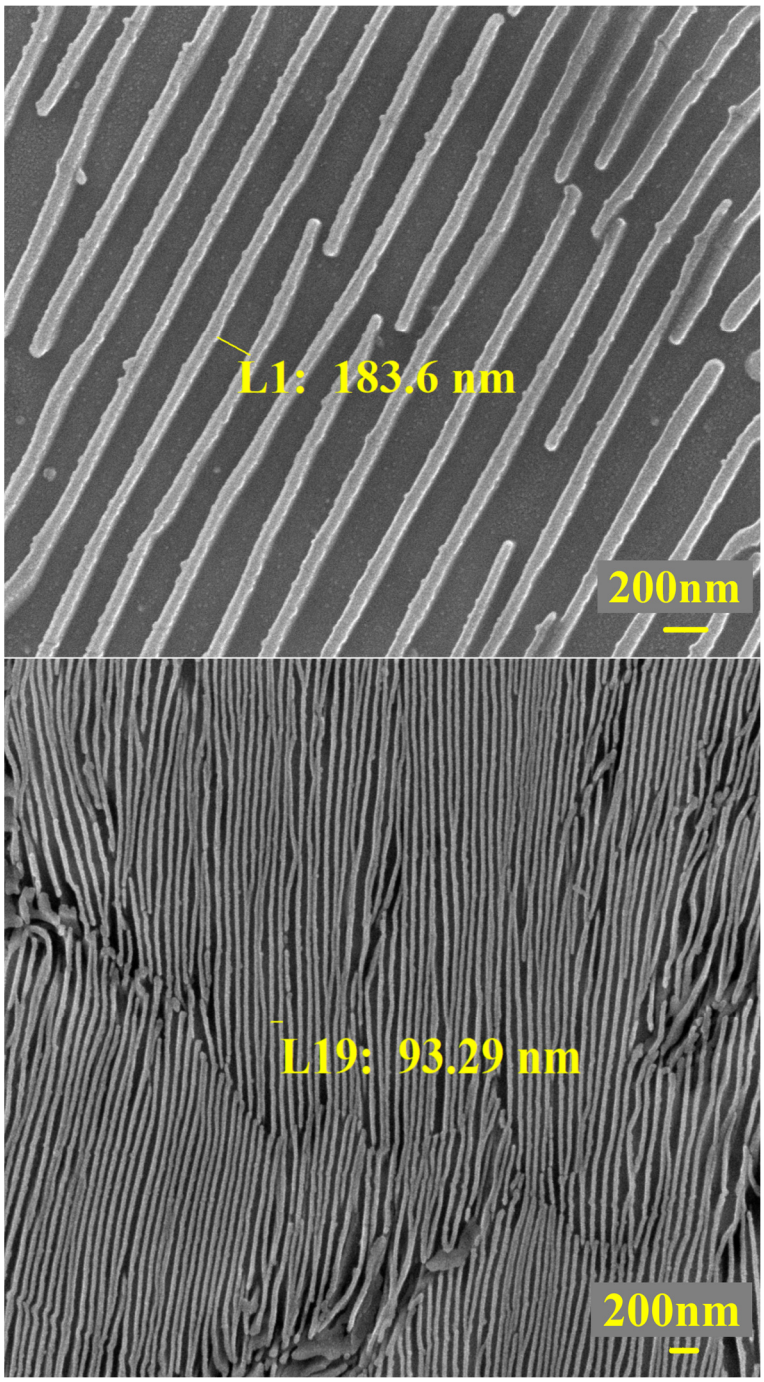

Figure 2. *Cont.*

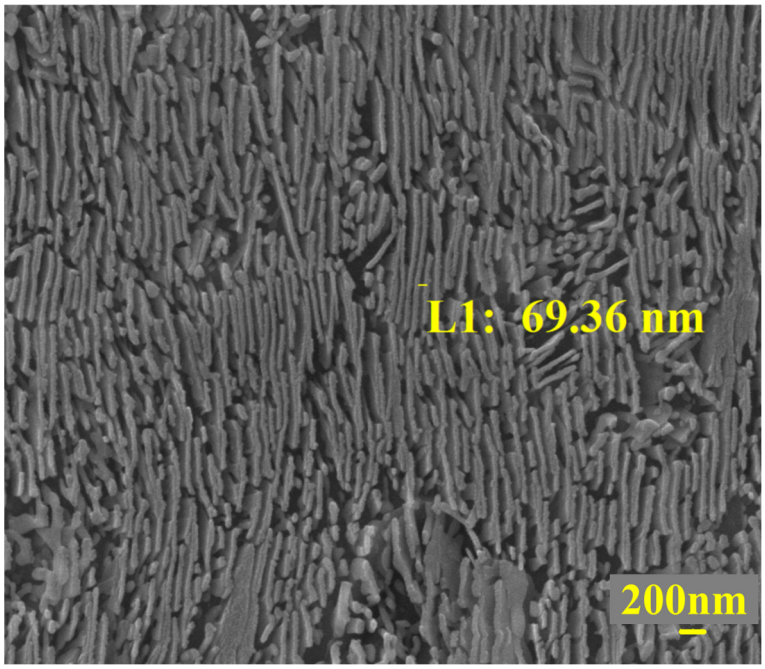

Figure 2. The morphology of typical pearlite, sorbite, and troostite.

For the purpose of achieving sorbite transformation, supercooled austenite must be cooled quickly to avoid coarse pearlite forming (the cooling rate is approximately 20~40 °C per second). However, it cannot be overcooled deeply, otherwise, the transformation temperature of the supercooled austenite may be in the region of bainite, and bainite will be produced (the strength and plastic toughness of bainite is relatively low; the strength is approximately 800~1200 MPa the plastic toughness is approximately 5~15%).

Furthermore, maintenance of a narrow temperature range within the pearlite transformation course is crucial to acquiring the sorbite microstructure. In the conventional Stelmor technique, noticeable temperature gradients from the wire core to the surface exist, caused by inadequate cooling speed [8–10]. For hypereutectoid steel, it will lead to composition segregation and the formation of proeutectoid cementite, which, in turn, triggers the formation of free ferrite. Using a salt bath can solve these shortcomings.

2.2. The Influence of Trace Elements on Sorbite Formation Rate

In actual production, adding the alloy elements can also improve the rate of sorbite formation. The advantages and disadvantages of adding each element and the general control range of each element content are shown in Table 2.

For every 0.01% increase in carbon mass fraction, the tensile strength can be increased by approximately 8 MPa. Carbon can effectively refine the interlamellar spacing of pearlite, thereby improving strength. However, excessive carbon causes the steel to transform into hypereutectoid steel, and the proeutectoid network secondary cementite will be precipitated before the austenite transformation to reduce the plasticity of the steel. Generally, the carbon content is controlled at 0.7~1.2%.

Solid solution strengthening of silicon can improve the strength of ferrite and the hardenability of steel. Si has low solubility in cementite and is enriched at the ferrite/cementite interface, which can reduce the spheroidization rate of cementite and alleviate the strength decline caused by the heat in the hot dip galvanizing stage. Si can reduce the segregation of C atom in ferrite lamella, so as to make its distribution more uniform and refine the lamellar spacing. However, too high Si is not conducive to the plasticity and toughness of the wire, and the general Si content should be controlled at 0.15~1.5%.

Table 2. Advantages and disadvantages of adding various elements [11].

Element	Advantage	Disadvantage	Content
C	Refining pearlite interlamellar spacing	High content will precipitate proeutectoid secondary cementite and reduce plasticity	0.7~1.2%
Si	Improve the strength of ferrite and the hardenability of steel	High content is not beneficial to the plasticity and toughness of the wire	0.15~1.5%
Mn	Alleviate the strength loss of wire caused by heating during hot dip galvanizing process	Segregation tendency is more obvious	<1%
Cr	Reducing the transformation temperature and refining the interlamellar spacing of pearlite	High content will cause the wire to break due to delamination during torsional deformation, reducing the strength of the wire.	0.03~0.5%
Ni	Improve the toughness of wire rods	High content will prolong the phase transformation time	0.1~0.5%
V	Precipitation strengthening to increase the strength of ferrite	High content will reduce the plasticity	<0.06%

The content of manganese in cementite is slightly higher than that in ferrite, mainly because Si solid solution in ferrite causes Mn to migrate into cementite. The enriched Mn in cementite enhances its stability. However, Mn has a significant segregation tendency, and it is generally recommended to control the Mn content below 1%.

The precipitation and strengthening of chromium can increase the strength of steel. Cr is beneficial to lower the transformation temperature and refine the interlamellar spacing. When its content increases, the transformation time will be prolonged, and martensite or bainite may be produced during hot rolling, which affects the performance of wire rods. In addition, the increase in Cr content will cause the wire to fracture due to delamination during torsional deformation, reducing the plasticity (the addition amount of Cr is generally 0.03~0.5%) [12].

Adding alloy elements raises the production costs and the difficulty of steelmaking, ironmaking, continuous casting, and rolling processes. Therefore, at present, improving the mechanical properties of wires should mainly start from the heat treatment process, rather than adding alloy elements.

3. Wire Heat Treatment Course in Steel Plants

In the wire cooling course, selecting appropriate cooling process conditions and cooling medium is critical in optimizing the performance of steel and determining its final quality. The principle of formulating cooling processes is to maintain the transformation temperature range of the microstructure as much as possible between 600 °C and 650 °C. Based on this, different steel plants employ various cooling coolants. At present, steel plants have adopted a variety of heat treatment methods for sorbite wires, including Stelmor air cooling, lead bath treatment, online salt bath quenching technology, offline salt bath quenching, and water bath cooling technology.

Figure 3 show the Stelmor air cooling technology. When processing large-size wire rods with a diameter of more than 16 mm using Stelmor, problems of uneven cooling will occur (the wire center is sparse and the temperature drop is rapid; the wire edge junction area is densely packed and the temperature drop is slow) and the cooling speed is slow (resulting in the formation of proeutectoid network cementite) [13,14]. In addition, when processing wires with diameters less than 6 mm using Stelmor, the cooling ability will be too strong and a brittle martensite structure will appear. These reasons all limit its ability to handle wire rods [11]. Wire rods produced on the Stelmor air-cooled line generally need to be re-austenitized and then subjected to heat treatment such as a salt bath or lead bath.

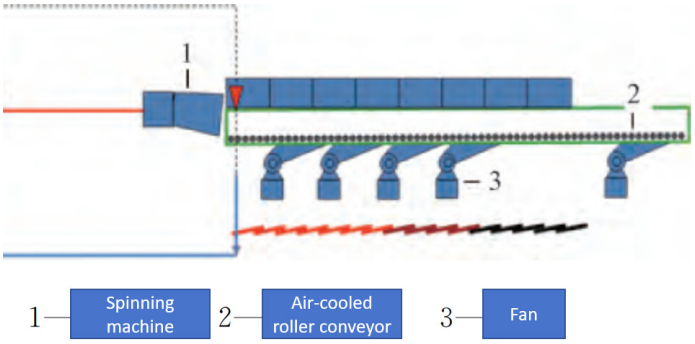

Figure 3. The Stelmor air cooling process [1].

Lead bath cooling (LP), an early sorbite treatment technology, has been widely used in the steel industry. However, this technology has some drawbacks. The primary problem is the toxicity of liquid lead, which may pose a serious threat to the health of operators. In addition, lead bath cooling is accompanied by high costs and serious environmental pollution problems [15,16].

Nippon Steel and Kobe Steel developed steel wires with a strength of 1770 MPa as early as the end of the 20th century. When these two companies produce 2000 MPa grade steel wires, their ideas are to increase the C content to improve strength and increase the Cr content to improve hardenability. However, when the content of C element is too high, it will transform into hypereutectoid steel. Before the austenite transformation, proeutectoid network secondary cementite will precipitate in the steel, which will affect the overall performance of the wire rod. Therefore, how to effectively eliminate this secondary cementite through heat treatment has become a problem that urgently needs to be studied and solved in depth. Yi H [17] conducted research in this regard. He designed a full-layered pearlite structure in a steel containing 0.4% C through slow cooling. The mechanism is that the larger austenite grain dimensions inhibit the formation of undesirable ferrite. Under the huge driving force, fine divorced cementite layers were formed in the pearlite, realizing the divorced eutectoid transformation under the non-eutectoid composition. Nippon Steel and Kobe Steel have also developed directline patenting (DLP) online salt bath process [18]. The DLP process cleverly uses the residual heat after rolling of the wire to carry out salt bath treatment, thereby achieving a structure and performance comparable to that of lead bath quenching.

In response to China's call for energy conservation, environmental protection, cost reduction, and efficiency improvement, Chinese steel companies have also conducted research on salt bath process technology and achieved good results.

In 2017, Qingdao Special Steel designed an offline salt bath sorbite treatment (QWTP) line. After salt bath treatment, the network carbides are eliminated, the sorbite rate is increased to 95%, and the sorbite sheet orientation is more consistent and the spacing is smaller. On the basis of offline salt bath, as shown in Figure 4, Qingdao Special Steel has also independently developed an online salt bath heat treatment process [19]. Online salt bath is a green and low-carbon new technology where, after wire rod laying, the bundled wire rods are directly placed into the salt bath following a brief air cooling. The strength and plasticity of the wire after being treated by online salt bath heat treatment are greatly improved (the tensile strength is 1215~1325 MPa and the reduction area is 40~48%). Compared with the traditional Stelmor air-cooling process, the online salt bath heat treatment technology significantly reduces the possibility of abnormal structure formation. This process not only improves the cooling effect of the wire but also effectively manipulates the temperature rise during the cooling course and promotes the phase transition to proceed in a lower temperature range.

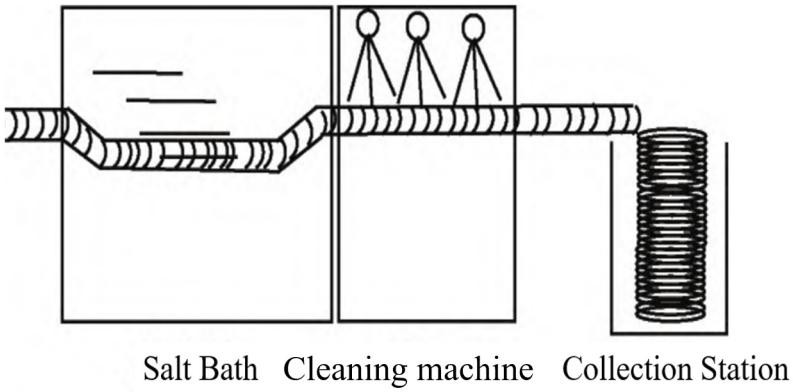

Figure 4. Online salt bath process [19].

As shown in Figure 5, Xingcheng Special Steel and An steel adopt green easy drawing conveyer (EDC) technology instead of the salt bath process [1,20], and the products have been used in the construction of the Shanghai–Tong Highway–Railway Bridge [21,22]. Water bath cooling relies on additives to manipulate the water film in the film boiling stage, making process control difficult. Low-concentration additives cool faster and tend to form martensite, while the phase transformation temperature of high-concentration additives increases compared with lead bath quenching, and the continuous change in cooling rate leads to uneven microstructure (the continuous variation in cooling rate makes it difficult to stably control the phase transformation temperature range within 600~650 °C) [23].

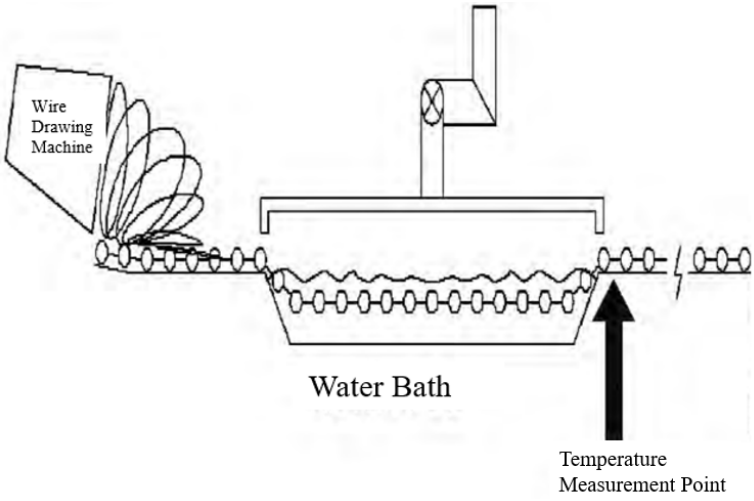

Figure 5. EDC water bath process [20].

As users increase their performance demands, the traditional Stelmor process is gradually turning to the technology of salt bath cooling. Compared with the Stelmor process, the edge and center of the wire are cooled relatively uniformly. The molten salt can prevent the wire from transforming into bainite and reduce the formation of abnormal structures (coarse pearlite, proeutectoid cementite, free ferrite, divorced pearlite, and martensite). Salt bath heat treatment allows accurate manipulation of the microstructure and properties of wire rods, so it has advantages in improving the strength, hardness, wear resistance, and corrosion resistance, is suitable for wire rods of various types of steel grades, and can adapt to wires of different diameters and shapes. Furthermore, salt bath heat treatment process parameters, i.e., the temperature of the salt bath, can be adjusted according to different wire requirements, so it has strong adaptability and flexibility.

4. Salt Bath Heat Treatment of Sorbite Wires

4.1. Advantages of Salt Bath Heat Treatment

The cooling medium of the salt bath has a low viscosity [24] and remains constant over a certain temperature range [25], improving the cooling properties [26,27]. There are two major types of quenched salts: nitrates/nitrites and chloride salts [28]. Quenching with hydroxides and carbonates is not suggested as these materials can be detrimental to the corrosion sensitivity of the surface [29]. Furthermore, to guarantee that all austenite experiences thorough sorbite transformation, a sufficiently long thermostatic zone must exist, which can avoid the formation of bainite. At present, selecting the suitable coolant and precisely manipulating the cooling effect are key points in molten salt bath cooling course.

Many scholars have used numerical simulation and physical simulation methods to conduct extensive research on the wire cooling course from the aspects of the wire phase transformation mechanism [30], wire sample quenching mechanism [31,32], and wire internal microstructure control [33], trying to clarify the wire cooling mechanism. The following two sections introduce the progress of simulation and experimental research on salt bath heat treatment.

4.2. Simulation of Wire Salt Bath Heat Treatment

The beginning temperature for supercooled austenite is an important parameter. Most researchers use an incubation period superposition method to compute this temperature [34]. The period from the cooling of supercooled austenite to the beginning of transformation is divided into many superpositions of micro time Δt, and the temperature is considered to be constant in each Δt. Using the TTT (T—time, T—temperature, T—transformation) curve, the percentage of Δt at each isothermal temperature to the total incubation period at that temperature can be obtained. When the time superposition equals 1, the incubation period is considered to end and the phase transformation begins.

After the phase transition begins, the main thing involved is the calculation of the phase transition fraction. Most scholars [35,36] still divide the phase transition process into superposition of many micro-time phase transitions. Every phase transition in a short time is considered to be an isothermal phase transition.

In the course of austenite cooling, the latent heat will affect the temperature field distribution. The latent heat release model has been studied for a long time. To predict the latent heat, Equation (1) has been applied to trace the course of diffusion phase transition as early as the 1930s [37–39], where X is the phase transition rate and b and n are time-dependent variables, which can be fitted utilizing the TTT curve.

$$X = 1 - \exp(-bt^n) \quad (1)$$

The calculation of the transition fraction and the latent heat is obtained by using the additivity rule of TTT curve. This model was initially developed by Scheil E [40] and, subsequently, many scholars conducted a lot of research on this model, mainly focusing on the following two aspects:

(1) As early as the 1980s, the phase transition from austenite to pearlite has been studied by applying the additive rule [41]; subsequently, the mathematical model describing the continuous cooling transition process has also been developed [42,43]. Then, the study about the influence of variables such as wire diameter, initial temperature, and heat exchange conditions on the wire temperature field [30,44], microstructure, and hardness distribution of steel appears [45]. Furthermore, it has been argued that the incubation time should also be taken into account in the calculating formula [46], while other scholars argue that only the phase transition stage follows Equation (1)

and the parameters of dynamics can be figured from the phase transition beginning time [35].

(2) Other scholars have studied and explained the application range of the additivity rule [47]. It is believed that the additivity rule can only be applied to non-rate-dependent processes (n in Equation (1) is a constant) [34] and the nucleation at the initial phase transition dominates the subsequent phase transition dynamics [36].

4.3. Experiment of Salt Bath Cooling Course

Most of the research on the salt bath treatment is to experimentally measure the various mechanical properties and microstructures of wires after heat treatment or simulate the heat treatment course by inverse heat transfer algorithm and TTT curve superposition method [48].

The heat transfer coefficient (HTC) is critical in salt bath isothermal quenching [49]. Some scholars [29,31,50] used the temperature data of sample obtained from the quenching experiment to calculate the HTC by using the inverse heat transfer algorithm [32] and noticed there are only nuclear boiling and convective heat transfer [51,52], as shown in Figure 6.

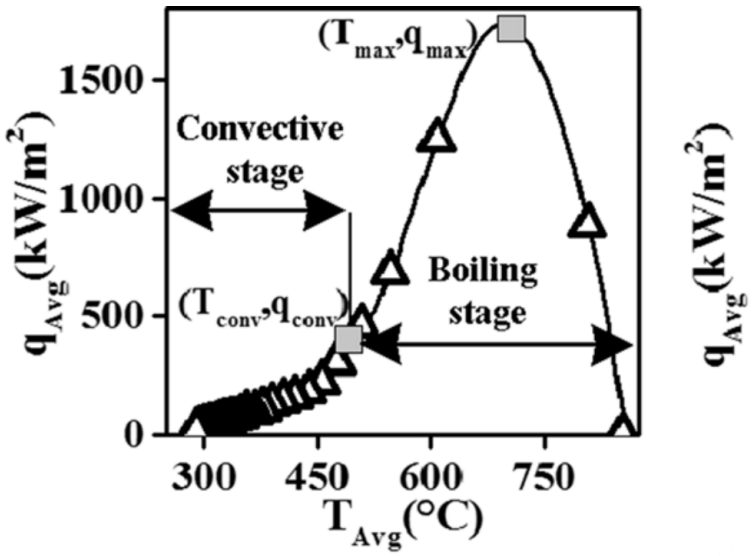

Figure 6. Heat exchange mechanism of salt bath cooling course [48].

By analyzing the experimental data obtained from water quenching experiments, some scholars [53] have studied the effects of adding agents on the cooling characteristics, vapor layering properties, and gas bubble kinetics by mean of experiment. After the removal of surfactants at higher temperatures, the salt adding agents showed better properties than deionized water.

4.4. Boiling Heat Transfer of Wire During Quenching

When the liquid is in touch with a surface whose temperature is greater than saturated temperature under corresponding pressure, the liquid will boil on the surface, which is named boiling heat transfer [54]. Depending on the liquid temperature during boiling, boiling heat transfer can be categorized into saturated and subcooled boiling. Depending on the size of the boiling space, boiling heat transfer can be categorized into pool boiling [55] and forced convection boiling [56]. Heat transfer in the salt bath belongs to forced convection boiling, also known as flow boiling, which includes both convection and boiling heat transfer [57].

The course of cooling the wire belongs to the flow boiling stage before the wire is cooled to 600 °C. At this stage, both the boiling of the salt bath and the forced convection heat transfer exist, which makes the heat transfer mechanism complicated. At this stage, the bubbles boiling on the heating wall will be influenced as a result of the additional flow of the fluid, resulting in changes in the original motion mechanism of the gas. Furthermore, because the liquid is continuously heated during flow, the flow state will change dynamically. The change of flow state will, in turn, act on the movement course of bubbles, thus increasing the complexity of the flow boiling heat exchange course [58,59]. At present, there is no theoretical formula that can explain flow boiling, but many researchers have conducted considerable studies on it [60,61]. For example, Lu M et al. [62] investigated the influence of the heat flux and refrigerant in a pipe on the heat transfer performance of two-phase flow boiling. It was discovered that nuclear boiling is the dominant heat exchange form in the lower dryness region and convection evaporation is the dominant heat exchange form in the higher dryness region. Both refrigerants show the same tendency with very slight differences in heat exchange.

In general, the heat transfer mechanism obtained by scholars through experimental research is quite different. For the study of flow boiling prediction method, in order to facilitate application, most scholars put forward some heat transfer correlation formulas [63]. For example, K and Likar S G [64], Bertsch S S [65], Gungor K and EWinterton R S [66,67], and Choi K [68] all developed experimental correlations to forcast flow boiling HTC in horizontal and vertical pipes, and mean deviations of their studies are 18.88%, less than 30%, around 20%, and 22.5%, respectively.

From the above studies, it can be found that the error of the prediction correlation formula of flow boiling is large, which is primarily because of the complicated heat exchange mechanism of flow boiling. Li W and Wu Z [69] analyze 3700 sets of data in 26 literatures, discover that the error of the existing correlation formula is very large, and the error of the smallest Lazarek–Black formula [70] reaches 36.94%.

In actual salt bath production, when the wire enters the molten salt bath, the wire temperature is above 900 °C, far exceeding the boiling point of the medium, so boiling and convection heat transfer exist at the same time. As the temperature of the wire gradually cools down, the heat exchange mechanism changes to convection heat transfer. The flow pattern, molten salt bath temperature, and salt boiling will affect the temperature field of the wire. None of the above scholars simulated the entire dynamical cooling course. Li J et al. [71–73] simulated the entire dynamical cooling course. Unlike other scholars who did not consider the latent heat in the inverse heat transfer process, they used the finite difference method to take into account the phase transition equation into this program. Then, on the basis of the computed HTC from experiment and the convection HTC from simulation, the superposition model was selected to compute the comprehensive HTC for the flow boiling area.

4.5. Agent in the Cooling Course

Molten salt is an excellent heat exchange and storing medium due to its good thermal conductivity, heat capacity, wide operating temperature, low viscosity, and high stability [74]. In addition to the good characteristics of molten salts, nitrates are also highly resistant to corrosion [75,76]. Because the pure nitrates have a relatively high melting point, mixed nitrates are commonly used commercially. In solar power generation systems, solar salt ($NaNO_3$-KNO_3, ratio 6:4) and hitec ($NaNO_3$-KNO_3-$NaNO_2$, ratio 7:53:40) are commonly used as heat exchange and thermal storing mediums. For salt bath heat treatment, the cooling effect of these two molten salts is also good. For the solar salt, the melting point is 240 °C, the decomposition temperature is 530~565 °C, the density is 1840 kg/m^3,

and the heat capacity is 1550 J/kg/°C. For the hitec salt, the melting point is 142 °C, the decomposition temperature is 450~540 °C, the density is 1790 kg/m^3, and the heat capacity is 1540 J/kg/°C [75].

At present, the five molten salts shown in Table 3 are mainly used in industry. Their advantages and disadvantages are shown in the table. Among them, the thermal physical parameters of nitrates have obvious advantages [77,78]. They have a low melting point, good thermal stability [79], easy long-term use in industry, low viscosity and easy flow [80], and low corrosiveness, which is beneficial to the health of operators [81].

Table 3. Characteristics of various types of molten salt [81].

Molten Salt	Advantages	Disadvantages
Nitrates	Good stability, low viscosity, corrosion resistance, low cost	Overheating is likely to occur during melting, and the thermal conductivity is low
Carbonates	Low cost, high density and heat of solution, corrosion resistance	Melting point as high as 800 °C, high viscosity, easy to decompose
Chlorides	Low cost and high heat capacity	Highly corrosive, easy to decompose, high melting point
Fluorides	Low repellency to metals and high melting heat	High melting point, low thermal conductivity, volume shrinkage
Sulfates	Low cost, high density, high boiling point, low saturated vapor pressure	High melting point and high viscosity

The research on nitrates mainly focuses on the following aspects: the melting point of molten salt decreases to below 140 °C [82], the decomposition temperature increases to above 650 °C, and the working temperature expands to 500–650 °C; the heat capacity increases to over 1600 J/(kg·°C) and the thermal conductivity increases to 0.6 W/(m·°C) through the use of additives [78–80,83–89]; and thermal stability and corrosion resistance research under various working conditions.

5. Conclusions

As bridges develop towards ultra-large span and light weight, the performance requirements for steel wires used in bridges will continue to increase. Ultra-high strength, narrow strength fluctuation range, high torsion performance, fatigue resistance, corrosion resistance, and resistance to lamellar tearing are bound to become the development direction of ultra-high-strength wire for bridges in the future.

During the cooling course of the wires, boiling and forced convection heat transfer exist simultaneously. It is difficult to directly use thermocouples to measure the wires' temperature variations. The experiments in the existing literature are all completed in the quenching furnace in the laboratory, which has limited understanding for cooling course in actual production. Therefore, in terms of salt bath simulation, models such as molten salt bath, wires, and molten salt pump need to be established to accurately describe the molten salt flow field around the wires. In terms of experiments, it is necessary to obtain the temperature change curve of the wires from entering the salt bath to leaving the salt bath through experiments so as to accurately establish a model describing the heat exchange mechanism between wires and molten salt.

The cooling effect at different temperatures on the wires vary greatly. It is advisable to separate the molten salt bath in three sections to distinguish the cooling, phase transformation, and heat preservation stage. This may allow for better control of the temperature change of the wire and obtain a sorbite wire with excellent performance.

The salt bath heat treatment can be further studied in the following two aspects in the future:

(1) Selection of molten salt:

There have been some studies on ternary and quaternary molten salts and additive molten salts. These molten salts have better heat capacity and thermal conductivity. Therefore, some experiments and numerical simulation studies should be carried out on the cooling effect of different molten salts.

(2) Internal structure control of wire rod:

According to microstructure control objectives, it is necessary to study how to improve the sorbitization rate, how to avoid the formation of abnormal structures, and how to minimize the forming of reticulated carbides. In order to avoid the formation of reticulated carbides, the dynamic recrystallization law of steel should be studied to formulate and optimize the rolling process. The precipitation of reticulated carbides is related to the carbon content, alloy content, and cooling rate. Through material thermodynamic and kinetic calculations, combined with thermal simulation analysis, the effect of carbon level, alloy content, and cooling rate on the precipitation of reticulated carbides can be studied and the prediction model for the precipitation of network carbides can be explored.

(3) The online salt bath:

For online salt baths, the focus is on researching and simulating their microstructure dynamics, dynamic temperature fields of the molten salt, flow fields, temperature fields of the wire rods, and mechanical properties. It is necessary to study and design the molten salt temperature, molten salt flow rate, salt bath length, wire rod speed, and the entry and exit temperatures of the wire rod sections based on the steel grade and diameter of the wire rods. Since the wire rods enter the salt bath directly in bundles, it is also essential to ensure the uniformity of the mechanical properties across the wire rod loops and to minimize the temperature difference between the lap points and the middle sections of the wire rods.

In the future, research and development efforts in narrow-range chemical composition control, rolling and heat treatment process control, microstructure, and performance uniformity control should be explored to improve product quality stability.

Author Contributions: Conceptualization, J.L., C.L., Y.L., B.W., and B.Z.; methodology, J.L., C.L., Y.L., B.W., and B.Z.; software, J.L., C.L., Y.L., and B.Z.; validation, J.L., C.L., Y.L., B.W., and B.Z.; formal analysis, J.L., C.L., Y.L., B.W., and B.Z.; investigation, J.L., C.L., Y.L., B.W., and B.Z.; resources, J.L., C.L., Y.L., B.W., and B.Z.; data curation, J.L., C.L., Y.L., B.W., and B.Z.; writing—original draft preparation, J.L.; writing—review and editing, J.L., C.L., Y.L., B.W., and B.Z.; visualization, J.L., C.L., Y.L., B.W., and B.Z.; supervision, J.L., C.L., Y.L., B.W., and B.Z.; project administration, J.L., C.L., Y.L., B.W., and B.Z.; funding acquisition, J.L., C.L., Y.L., B.W., and B.Z. All authors have read and agreed to the published version of the manuscript.

Funding: This research received no external funding.

Data Availability Statement: Not applicable.

Conflicts of Interest: Authors Jun Li, Chuanmin Li, Yafeng Liu and Ben Zhang were employed by the company MCC Capital Engineering & Research Incorporation Limited. The remaining authors declare that the research was conducted in the absence of any commercial or financial relationships that could be construed as a potential conflict of interest. The company had no role in the design of the study; in the collection, analyses, or interpretation of data; in the writing of the manuscript, or in the decision to publish the results.

References

1. Sun, Z.; Chrn, H.; Zhang, J.; Bai, Y.; Xu, X. Production status analysis of wire rod for high strength bridge cable. *China Metall.* **2019**, *29*, 66–69.
2. You, X. Design and construction of Jujia Bridge in South Korea. *World Bridges* **2014**, *42*, 1–5.

3. Ridley, N. A review of the data on the interlamellar spacing of pearlite. *Metall. Mater. Trans. A* **1984**, *15A*, 1019–1036. [CrossRef]
4. An, K.S.; Jeong, S.W.; Bea, H.J.; Nam, W.J. Formation of abnormal structures and their effects on the ductility of eutectoid steel. *Met. Mater. Int.* **2016**, *22*, 995–1002. [CrossRef]
5. Xu, X. Discussion of Sorbitizing Process of Steel Wire. *Dongbei Spec. Steel* **2008**, *10*, 29–37.
6. Buono, V.L.; Gonzalez, B.M.; Lima, T.M.; Andrade, M.S. Measurement of fine pearlite interlamellar spacing by atomic force microscopy. *J. Mater. Sci.* **1997**, *32*, 1005–1008. [CrossRef]
7. Liu, T. *Metals and Heat Treatment*; Metallurgical Industry Press: Beijing, China, 2009.
8. Hong, L.; Wang, B.; Feng, S.; Yang, Z.; Yu, Y.; Peng, W.; Zhang, J. A three-dimensional mathematical model to predict air-cooling flow and temperature distribution of wire loops in the Stelmor air-cooling system. *Appl. Therm. Eng.* **2017**, *116*, 766–776. [CrossRef]
9. Huang, J.; Wang, B.; Xue, F.; Liu, S.; Hong, L.; Yu, Y.; Zhang, J. Effect of controlled cold air distribution on temperature profile and phase transformation of wire loops in the Stelmor air-cooling process. *Appl. Therm. Eng.* **2018**, *143*, 340–349. [CrossRef]
10. Hwang, J. Effects of nozzle shape and arrangement on the cooling performance of steel wire rod in the Stelmor cooling process. *Appl. Therm. Eng.* **2020**, *164*, 114461. [CrossRef]
11. Feng, L.; Wu, K.; Lu, X.; Qiao, W. Research Status and Development Tendency of Ultra-High Strength Steel Wire for Bridge Cables. *Mater. China* **2020**, *39*, 395–403.
12. Zhou, L.; Wang, L.; Chen, H.; Xie, Z.; Fang, F. Effects of chromium additions upon microstructure and mechanical properties of cold drawn pearlitic steel wires. *J. Mater. Eng. Perform.* **2018**, *27*, 3619–3628. [CrossRef]
13. Morales, R.D.; Lopéz, A.G.; Olivares, I.M. Mathematical simulation of Stelmor process. *Ironmak. Steelmak.* **1991**, *18*, 128–138.
14. Yu, W.-H.; Chen, S.-H.; Kuang, Y.-H.; Cao, K.-C. Development and application of online Stelmor controlled cooling system. *Appl. Therm. Eng.* **2009**, *29*, 2949–2953. [CrossRef]
15. Yoshie, A.; Sugimaru, S.; Nishida, S. New wire rods produced by inline heat treatment. *Nippon Steel Tech. Rep.* **1999**, *80*, 26–31.
16. Ohba, H.; Nishida, S.; Tarui, T.; Yoshimura, K.; Sugimoto, M.; Matsuoka, K.; Hikita, N.; Toda, M. High-performance wire rods produced with DLP. *Nippon Steel Tech. Rep.* **2007**, *96*, 50–56.
17. Yi, H. Full pearlite obtained by slow cooling in medium carbon steel. *Mater. Sci. Eng. A* **2010**, *527*, 7600–7604. [CrossRef]
18. Okonogi, M.; Yamazaki, K. Development of medium carbon steel wire rods for cold heading by isothermal transformation treatment. *Nippon Steel Sumitomo Met. Tech. Rep.* **2017**, *116*, 65–70.
19. Li, Y.; Zhen, X.; Wang, G.; Zhen, T.; Xu, K. High performance Fe-C-Mn-Si high carbon steel wire rod produced by in-line salt bath heat treatment. *China Metall.* **2023**, *33*, 104–110.
20. Che, A.; Ren, Y.; Han, L. Study on EDC controlled cooling technology for wire rod production. *Met. Prod.* **2016**, *42*, 35–39.
21. Wu, Y.; Ya, G.; Dai, X.; Zhang, X. Key techniques of 1960 MPa steel wire and wire strand for main cable of second humen bridge. *Bridge Constr.* **2018**, *48*, 6–10.
22. Yan, Z.; Xue, H. Test research on 2000 MPa 7 mm diameter steel wire for hutong changjiang river bridge. *J. China Railw. Soc.* **2018**, *40*, 115–119.
23. Han, L.; Ren, Y.; Bai, X.; Che, A. Development of high speed wire rod online water bath treatment technology. *Met. Prod.* **2014**, *40*, 40–43.
24. Sudheer, R.; Prabhu, K.N. A computer aided cooling curve analysis method to study phase change materials for thermal energy storage applications. *Mater. Des.* **2016**, *95*, 198–203. [CrossRef]
25. Peng, Q.; Ding, J.; Wei, X.; Yang, J.; Yang, X. The preparation and properties of multi-component molten salts. *Appl. Energy* **2010**, *87*, 2812–2817. [CrossRef]
26. Ramesh, G.; Prabhu, K.N. Comparative study of wetting and cooling performance of polymer–salt hybrid quench medium with conventional quench media. *Exp. Heat Transf.* **2015**, *28*, 464–492. [CrossRef]
27. Han, Y.; Lan, J.; Liu, X.; Shi, W. Advances in molecular dynamics studies of molten salts based on machine learning. *Acta Chim. Sin.* **2023**, *81*, 1663–1672. [CrossRef]
28. Chen, F.; Wen, Y.; Guo, Y.; Zheng, F.; Wang, S.; Yang, L.; Zheng, Y.; Li, D.; Ren, Y. Research status of viscosity characteristics of chlorinated molten salt system. *Inorg. Chem. Ind.* **2022**, *54*, 1–5.
29. Rao, K.P.; Prabhu, K.N. A comparative study on cooling performance of hot oil and molten salt quench media for industrial heat treatment. *J. Mater. Eng. Perform.* **2020**, *29*, 3494–3501. [CrossRef]
30. Serajzadeh, S. Prediction of temperature distribution and phase transformation on the run-out table in the process of hot strip rolling. *Appl. Math. Model.* **2003**, *27*, 861–875. [CrossRef]
31. Pranesh Rao, K.M.; Narayan Prabhu, K. Effect of bath temperature on cooling performance of molten eutectic $NaNO_3$-KNO_3 quench medium for martempering of steels. *Metall. Mater. Trans. A* **2017**, *48A*, 4895–4904. [CrossRef]
32. Ramesh, G.; Prabhu, K.N. Spatial dependence of heat flux transients and wetting behavior during immersion quenching of inconel 600 probe in brine and polymer media. *Metall. Mater. Trans. B* **2014**, *45*, 1355–1369. [CrossRef]

33. Guo, L.; Xu, K.; Gao, Y.; Sun, Q.; Niu, B. Effect of Salt Bath Isothermal Heat Treatment on Structure and properties of Ultra High Strength Hard Wire 100Si Steel. *Spec. Steel* **2023**, *44*, 84–89.
34. Lusk, M.; Jou, H.J. On the rule of additivity in phase transformation kinetics. *Metall. Mater. Trans. A* **1996**, *28A*, 287–291. [CrossRef]
35. Hawbolt, E.B.; Chau, B.; Brimacombe, J.K. Kinetics of austenite-ferrite and austenite-pearlite transformations in a 1025 carbon steel. *Metall. Mater. Trans. A* **1985**, *16A*, 565–578. [CrossRef]
36. Kuban, M.B.; Jayaraman, R.; Hawbolt, E.B.; Brimacombe, J.K. An assessment of the additivity principle in predicting continuous-cooling austenite-to-pearlite transformation kinetics using isothermal transformation data. *Metall. Mater. Trans. A* **1986**, *17*, 1493–1503. [CrossRef]
37. Johnson, W.A. Reaction kinetics in processes of nucleation and growth. *Trans. Trans. Am. Inst. Min. Metall. Eng.* **1939**, *135*, 416–422.
38. Avrami, M. Kinetics of phase change. I general theory. *J. Chem. Phys.* **1939**, *7*, 1103–1112. [CrossRef]
39. Kolmogorov, A.N. *On the Statistical Theory of Metal Crystallization*; Springer: Dordrecht, The Netherlands, 1992; pp. 188–192.
40. Scheil, E. Anlaufzeit der austenitumwandlung. *Arch. Für Das Eisenhüttenwesen* **1935**, *8*, 565–567. [CrossRef]
41. Umemoto, M.; Nishioka, N.; Tamura, I. Prediction of hardenability from isothermal transformation diagrams. *J. Heat Treat.* **1981**, *2*, 130–138. [CrossRef]
42. Kirkaldy, J.S.; Sharma, R.C. A new phenomenology for steel it and CCT curves. *Scr. Metall.* **1982**, *16*, 1193–1198. [CrossRef]
43. Kirkaldy, J.S.; Smith, P.N.; Sharma, R.C. Diffusion of manganese in paramagnetic BCC iron. *Metall. Trans.* **1973**, *4*, 624–625. [CrossRef]
44. Agarwal, P.K.; Brimacombe, J.K. Mathematical model of heat flow and austenite-pearlite transformation in eutectoid carbon steel rods for wire. *Metall. Mater. Trans. B* **1981**, *12B*, 121–133. [CrossRef]
45. Kakhki, M.E.; Kermanpur, A.; Golozar, M. Numerical simulation of continuous cooling of a low alloy steel to predict microstructure and hardness. *Model. Simul. Mater. Sci. Eng.* **2009**, *17*, 045007. [CrossRef]
46. Umemoto, M.; Horiuchi, K.; Tamura, I. Transformation kinetics of bainite during isothermal holding and continuous cooling. *Tetsu-Hagane* **1982**, *68*, 461–470. [CrossRef]
47. Verdi, C.; Visintin, A. A mathematical model of the austenite-pearlite transformation in plain carbon steel based on the Scheil's additivity rule. *Acta Metall.* **1987**, *35*, 2711–2717. [CrossRef]
48. Sugianto, A.; Narazaki, M.; Kogawara, M.; Shirayori, A. A comparative study on determination method of heat transfer coefficient using inverse heat transfer and iterative modification. *J. Mater. Process. Technol.* **2009**, *209*, 4627–4632. [CrossRef]
49. Zhang, C.; Han, S.; Wu, Y.; Zhang, C.; Guo, H. Investigation on convection heat transfer performance of quaternary mixed molten salt based nanofluids in smooth tube. *Int. J. Therm. Sci.* **2022**, *177*, 107534. [CrossRef]
50. Rao, K.P.; Prabhu, K.N. Compositional and bath temperature effects on heat transfer during quenching in molten $NaNO_3$–KNO_3 salt mixtures. *J. Mater. Eng. Perform.* **2020**, *29*, 1860–1868. [CrossRef]
51. Yagov, V.; Zabirov, A.; Kaban'Kov, O.; Minko, M. Heat transfer during cooling of high temperature spheres in subcooled water at different pressures. *Int. J. Heat Mass Transf.* **2017**, *110*, 219–230. [CrossRef]
52. Babu, K.; Prasanna Kumar, T.S. Comparison of austenite decomposition models during finite element simulation of water quenching and air cooling of AISI 4140 steel. *Metall. Mater. Trans.* **2014**, *45B*, 1530–1544. [CrossRef]
53. Inbaoli, A.; Kumar, C.S.; Jayaraj, S. Experimental investigation on the effect of additives on different orientations of Al6061 cylindrical sample during immersion quenching. *Appl. Therm. Eng.* **2022**, *204*, 118030. [CrossRef]
54. Xu, J. *Boiling Heat Transfer and Gas-Liquid Two-Phase Flow*; Atomic Energy Press: Beijing, China, 2001.
55. Ding, T.; Yang, G.; Chen, K.; Fan, G.; Meng, Z.; Yan, C.; Zhang, K.; Chen, H. Heat transfer evaluation of saturated pool boiling outside slender tube bundle in passive residual heat removal system of molten salt reactor. *Ann. Nucl. Energy* **2022**, *169*, 108963.
56. Shu, M.; Wang, Z. *Priciple and Design of Heat Exchangers*; Southeast University Press: Nanjing, China, 1996.
57. Ni, S.; Pan, C.; Hibiki, T.; Zhao, J. Applications of nucleate boiling in renewable energy and thermal management and recent advances in modeling—A review. *Energy* **2023**, *289*, 129962. [CrossRef]
58. Zhang, J.; Chang, H. *Heat Transfer*; Science Press: Beijing, China, 2009.
59. Qi, S.; Zhang, P.; Wang, R. Review of liquid nitrogen flow boiling heat transfer. *Cryogenics* **2006**, *34*, 417–423.
60. Greco, A.; Vanoli, G.P. Flow-boiling of R22, R134a, R507, R404A and R410A inside a smooth horizontal tube. *Int. J. Refrig.* **2005**, *28*, 872–880. [CrossRef]
61. Aprea, C.; Greco, A.; Rosato, A. Comparison of R407C and R417A heat transfer coefficients and pressure drops during flow boiling in a horizontal smooth tube. *Energy Convers. Manag.* **2008**, *49*, 1629–1636. [CrossRef]
62. Lu, M.; Tong, J.; Wang, C. Investigation of the two-phase convective boiling of HFO-1234yf in a 3.9 mm diameter tube. *Int. J. Heat Mass Transf.* **2013**, *65*, 545–551. [CrossRef]
63. Hamdar, M.; Zoughaib, A.; Clodic, D. Flow boiling heat transfer and pressure drop of pure HFC-152a in a horizontal mini-channel. *Int. J. Refrig.* **2010**, *33*, 566–577. [CrossRef]

64. Kandlikar, S.G. A general correlation for saturated two-phase flow boiling heat transfer inside horizontal and vertical tubes. *J. Heat Transf.* **1990**, *112*, 219–228. [CrossRef]
65. Bertsch, S.S.; Groll, E.A.; Garimella, S.V. A composite heat transfer correlation for saturated flow boiling in small channels. *Int. J. Heat Mass Transf.* **2009**, *52*, 2110–2118. [CrossRef]
66. Gungor, K.E.; Winterton, R.S. Simplified general correlation for saturated flow boiling and comparisons of correlations with data. *Chem. Eng. Res. Des.* **1987**, *65*, 148–156.
67. Liu, Z.; Winterton, R.H.S. A general correlation for saturated and subcooled flow boiling in tubes and annuli, based on a nucleate pool boiling equation. *Int. J. Heat Mass Transf.* **1991**, *34*, 2759–2766. [CrossRef]
68. Choi, K.; Chien, N.; Oh, J. Heat transfer coefficient during evaporation of R-1234yf, R-134a, and R-22 in horizontal circular small tubes. *Adv. Mech. Eng.* **2013**, *5*, 132397. [CrossRef]
69. Li, W.; Wu, Z. A general criterion for evaporative heat transfer in micro/mini-channels. *Int. J. Heat Mass Transf.* **2010**, *53*, 1967–1976. [CrossRef]
70. Lazarek, G.; Black, S. Evaporative heat transfer, pressure drop and critical heat flux in a small vertical tube with R-113. *Int. J. Heat Mass Transf.* **1982**, *25*, 945–960. [CrossRef]
71. Li, J.; Wang, B.; Zhang, J. A Novel Design of a Molten Salt Bath Structure and Its Quenching Effect on Wire Transformation from Austenite to Sorbite. *Metals* **2024**, *14*, 483. [CrossRef]
72. Li, J.; Wang, L.; Wang, R.; Zhang, Y.; Wang, B.; Zhang, J. Controlling the Optimal Phase Transition Temperature of Wires during Quenching in Salt Bath through Process Parameters. *Mater. Today Commun.* **2024**, *40*, 109379. [CrossRef]
73. Li, J.; Wang, L.; Xing, C.; Zhang, Y.; Wang, B.; Zhang, J. Effect of inflow mode and parameters on temperature and phase transition of wires during isothermal quenching in molten salt bath. *Metall. Mater. Trans. B* **2024**, *55*, 301–318. [CrossRef]
74. Li, X.; Wu, S.; Wang, Y.; Xie, L. Experimental investigation and thermodynamic modeling of an innovative molten salt for thermal energy storage (TES). *Appl. Energy* **2018**, *212*, 516–526. [CrossRef]
75. Sun, L. Experimental Research on Molten Salt Corrosion Property and Optimization. Ph.D. Thesis, Beijing University of Technology, Beijing, China, 2007.
76. Zhai, W.; Yang, B.; Huang, G.; Wang, Z.; Li, S. Preparation and properties of mixed nitrite molten salts. *Inorg. Chem. Ind.* **2019**, *51*, 33–38.
77. Wilson, C.J.; Kramer, C.M. The phase diagram of $NaNO_3$—KNO_3. *Thermochim. Acta* **1980**, *42*, 253–264.
78. Mahan, A.; Mishra, A. Thermodynamic studies of ternary eutectic mixture KNO_3+$NaNO_2$+$NaNO_3$ at different temperatures. *J. Indian Chem. Soc.* **2008**, *85*, 105–107.
79. Tufeu, R.; Petitet, J.P.; Denielou, L.; Le Neindre, B. Experimental determination of the thermal conductivity of molten pure salts and salt mixtures. *Int. J. Thermophys.* **1985**, *6*, 315–330. [CrossRef]
80. Shukla, R.K.; Dwivedi, S.; Awasthi, P. Temperature dependent study of viscosity of KNO_3–$NaNO_2$–$NaNO_3$ ternary molten salts. *Phys. Chem. Liq.* **2006**, *44*, 431–440. [CrossRef]
81. Ma, L.; Zhang, C.; Wu, Y.; Lu, Y. Comparative review of different influence factors on molten salt corrosion characteristics for thermal energy storage. *Sol. Energy Mater. Sol. Cells* **2022**, *235*, 111485. [CrossRef]
82. Alexander, J.; Hindin, S.G. Phase relations in heat transfer salt systems. *Indengchem* **2002**, *39*, 1044–1049. [CrossRef]
83. Fernández, A.; Ushak, S.; Galleguillos, H.; Pérez, F. Development of new molten salts with $LiNO_3$ and $Ca(NO_3)_2$ for energy storage in CSP plants. *Appl. Energy* **2014**, *119*, 131–140. [CrossRef]
84. Fernández, A.; Ushak, S.; Galleguillos, H.; Pérez, F. Thermal characterisation of an innovative quaternary molten nitrate mixture for energy storage in CSP plants. *Sol. Energy Mater. Sol. Cells* **2015**, *132*, 172–177. [CrossRef]
85. Wang, T.; Mantha, D.; Reddy, R.G. Thermal stability of the eutectic composition in $LiNO_3$–$NaNO_3$–KNO_3 ternary system used for thermal energy storage. *Sol. Energy Mater. Sol. Cells* **2012**, *100*, 162–168. [CrossRef]
86. Wang, T.; Mantha, D.; Reddy, R.G. Novel low melting point quaternary eutectic system for solar thermal energy storage. *Appl. Energy* **2013**, *102*, 1422–1429. [CrossRef]
87. Takahashi, Y.; Sakamoto, R.; Kamimoto, M. Heat capacities and latent heats of $LiNO_3$, $NaNO_3$, and KNO_3. *Int. J. Thermophys.* **1988**, *9*, 1081–1090. [CrossRef]
88. Zhen, X.; Li, Y.; Wang, G.; Hou, J.; Zheng, T. Effect of cooling process after hot-rolling on microstructure and drawing property of wire rod for high strength welding wire. *Heat Treat. Met.* **2023**, *48*, 176–181.
89. Gu, S.; Sun, M.; Wang, B.; Zhang, J. Simulation and experimental study of fluid flow and solidification behavior in thin slabs continuous casting process under secondary electromagnetic stirring. *Steel Res. Int.* **2024**, *95*, 2300398. [CrossRef]

Disclaimer/Publisher's Note: The statements, opinions and data contained in all publications are solely those of the individual author(s) and contributor(s) and not of MDPI and/or the editor(s). MDPI and/or the editor(s) disclaim responsibility for any injury to people or property resulting from any ideas, methods, instructions or products referred to in the content.